



Mechanical Characterization Study of Sintered Silver Pastes

Preprint

Paul Paret, Joshua Major, Douglas DeVoto
and Sreekant Narumanchi
National Renewable Energy Laboratory

Yansong Tan and Guo-Quan Lu
Virginia Polytechnic Institute and State University

*Presented at American Society of Mechanical Engineers (ASME)
2018 International Technical Conference and Exhibition on
Packaging and Integration of Electronic and Photonic Microsystems
(InterPACK 2018)
San Francisco, California
August 27–30, 2018*

Suggested Citation

Paul Paret, Joshua Major, Douglas DeVoto, Sreekant Narumanchi, Yansong Tan, and Guo-Quan Lu. 2018. "Mechanical Characterization Study of Sintered Silver Pastes: Preprint." Golden, CO: National Renewable Energy Laboratory. NREL/CP-5400-71381. <https://www.nrel.gov/docs/fy19osti/71381.pdf>.

**NREL is a national laboratory of the U.S. Department of Energy
Office of Energy Efficiency & Renewable Energy
Operated by the Alliance for Sustainable Energy, LLC**

This report is available at no cost from the National Renewable Energy Laboratory (NREL) at www.nrel.gov/publications.

Conference Paper
NREL/CP-5400-71381
October 2018

Contract No. DE-AC36-08GO28308

NOTICE

This work was authored in part by the National Renewable Energy Laboratory, operated by Alliance for Sustainable Energy, LLC, for the U.S. Department of Energy (DOE) under Contract No. DE-AC36-08GO28308. Funding provided by the U.S. Department of Energy Office of Energy Efficiency and Renewable Energy Vehicle Technologies Office. The views expressed in the article do not necessarily represent the views of the DOE or the U.S. Government. The U.S. Government retains and the publisher, by accepting the article for publication, acknowledges that the U.S. Government retains a nonexclusive, paid-up, irrevocable, worldwide license to publish or reproduce the published form of this work, or allow others to do so, for U.S. Government purposes.

This report is available at no cost from the National Renewable Energy Laboratory (NREL) at www.nrel.gov/publications.

U.S. Department of Energy (DOE) reports produced after 1991 and a growing number of pre-1991 documents are available free via www.OSTI.gov.

Cover Photos by Dennis Schroeder: (left to right) NREL 26173, NREL 18302, NREL 19758, NREL 29642, NREL 19795.

NREL prints on paper that contains recycled content.

MECHANICAL CHARACTERIZATION STUDY OF SINTERED SILVER PASTES BONDED IN A DOUBLE-LAP CONFIGURATION

Paul Paret

National Renewable Energy
Laboratory
Golden, CO, USA
Paul.Paret@nrel.gov

Joshua Major

National Renewable Energy
Laboratory
Golden, CO, USA

Douglas DeVoto

National Renewable Energy
Laboratory
Golden, CO, USA

Sreekant Narumanchi

National Renewable Energy
Laboratory
Golden, Colorado, USA

Yansong Tan

Virginia Polytechnic Institute and
State University
Blacksburg, VA, USA

Guo-Quan Lu

Virginia Polytechnic Institute
and State University
Blacksburg, VA, USA

ABSTRACT

Sintered silver-based bonded interfaces are a critical enabling technology for high-temperature, compact, high-performance, and reliable wide-bandgap packages and components. High-pressure (~40 MPa) sintered silver interfaces have been implemented commercially, most notably the commercial products offered by Semikron. To reduce manufacturing complexity, there is significant industry interest in pressure-less sintered silver interfaces. To this end, current formulations of sintered silver paste are comprised of purely nano-sized silver particles or a combination of nano- and micro-sized silver particles/flakes. It is essential to quantify the mechanical properties and determine the reliability of these interfaces prior to use in automotive power electronics applications. In this paper, research efforts at the National Renewable Energy Laboratory, in collaboration with Virginia Polytechnic Institute and State University and an industry partner, in optimizing the synthesis procedure and mechanical characterization of sintered silver double-lap samples are described. These double-lap samples were synthesized using pressure-less sintering techniques. Shear testing was conducted at multiple temperatures and displacement rates on these samples sintered using two types of sintered silver pastes, one of them consisting of nano-silver particles and the other a hybrid paste or a combination of nano- and micron-sized silver flakes, employed in a double-lap configuration. Maximum values of shear stress obtained from the characterization study are reported.

INTRODUCTION

Power electronics packaging in the rapidly growing power industry is becoming more critical than ever before. To improve performance, reduce volume and weight, and get higher efficiency out of electronics packages, wide-bandgap devices such as silicon carbide (SiC) and gallium nitride were proposed as a replacement for widely used silicon (Si) devices. A redesign of the traditional packaging for power modules, both in materials and design, is necessary to exploit the faster switching speed and to enable high-temperature operation of the wide-bandgap devices. For high-temperature operation

(>200°C), materials that can withstand severe thermo-mechanical stresses and function without any failure for long periods of time need to be considered. In particular, for bonded interfaces, i.e., die-attach and substrate-attach, reliable operation at elevated temperatures is a major challenge as a failure would eventually result in a thermal runaway of the entire power electronics package.

Traditionally, solders have predominantly been used as interface materials in power electronics packages in the automotive industry. With the push towards replacing Si with wide-bandgap devices, high-temperature-compatible materials have gained significant interest. Among these materials, sintered silver, along with transient liquid-phase bonding, is a leading candidate for replacing solders in novel power electronics packaging designs. In the past, sintered silver made from micron-sized silver particles demonstrated excellent reliability under accelerated thermal cycling conditions [1]. However, the drawback of the high bonding pressure (30 – 40 MPa) requirement resulted in its limited applications and necessitated the research and development of novel and simple bonding techniques of sintered silver. To this end, sintered silver paste comprising nano-silver particles were developed [2] and more recently, hybrid sintered silver paste, involving a mixture of nano- and micron-sized silver particles/flakes, are gaining traction among various researchers and the industry. With these formulations, sintering can be achieved through purely a temperature-driven diffusion of the silver particles without applying any pressure. While micron-sized sintered silver paste has made inroads into commercial power electronics packages [3], more work is required to establish the mechanical properties and thermomechanical reliability of large-area pressure-less sintered silver pastes before adopting them for commercial applications. A comprehensive review of the different types of sintered silver pastes available in the industry is provided by Siow [4]. In this study, the merits and demerits of different types of sintered silver pastes available in the industry are compared and the author predicts that these pastes will become mainstream in the power electronics and microelectronics packaging industry over the next few years.

A common test method used to measure the integrity and strength of a bonded interface material is the shear stress test. In the past few years, several studies were conducted to determine the shear strength and other mechanical properties of sintered silver joints. Khazaka et al. [5] conducted a detailed study reviewing the different sintering parameters that affect the shear strength of nano-silver joints. A comprehensive literature survey of the reliability studies performed by various researchers is also provided. The authors attribute the variation in reported electrical, thermal, and mechanical properties of sintered silver in the literature to the microstructural variation of the material being tested, mainly material density and grain size. A similar study was conducted by Li et al. [6] on samples fabricated by bonding multiple SiC dies on direct-bond-copper substrates. Bond line thickness, substrate metallization, and synthesis pressure were varied among the different tested samples. In another study to determine the mechanical properties of sintered silver comprising micron-sized silver particles, Caccuri et al. [7] synthesized bulk specimens with similar microstructure and investigated the effect of joint density on its mechanical properties. Kahler et al. [8] worked on a sintered silver paste comprising a mixture of both micron-sized and nano-sized particles and achieved shear strength values close to 40 MPa. Chua et al. [9] characterized the evolution of porosity and microstructure of pressure-less sintered nano-silver joints bonded on direct-bond-copper, copper-plated, and silver-plated substrates. Test samples were aged at 300°C for 1,000 hours, and shear strength was measured. In a similar study [10], Egelkraut et al. investigated the impact of thermal aging on the shear strength and microstructural evolution of nano-silver pastes and compared it to other high-temperature solder alloys.

In addition to shear test, another key aspect of a bonded interface material developed for electronics packaging applications, especially at high temperatures, is thermomechanical reliability. Similar to the study on mechanical characterization, research on assessing the thermomechanical reliability of sintered silver joints provides critical information to power module manufacturers and electronics packaging design engineers. Work on this end has increased in the past few years as indicated by the rising number of publications highlighting the thermomechanical reliability of sintered silver joints. Bai and Lu [11] conducted a thermal cycling experiment between 50°C and 250°C on 1.706 mm x 1.380 mm dies bonded to silver- and gold-plated direct-bond-copper substrates, where the samples survived for 4,000 and 6,000 cycles, respectively. This study considered a 50% drop in shear strength as the failure criterion. Zhao et al. [12] studied the impact of thermal aging on the shear strength of sintered nano-silver joints using 13.5 mm x 13.5 mm Si chips bonded on a bare copper plate. Knoerr et al. [13] performed thermal cycling and power cycling accelerated tests on sintered nano-silver joints made with different sintering parameters and developed a lifetime prediction model using the Coffin-Manson

approach. The footprint of the samples was 14 mm x 14 mm, and 20% growth in the crack area was considered to be the failure criterion. Rajaguru et al. [14] developed a computational design optimization model of a power electronics module to improve the reliability of its sintered silver joint at the interface between a SiC chip and the substrate. In this work, a reduced-order modeling approach was adopted to analyze the impact of design variations on the reliability of the sintered silver joint. Henaff et al. [15] formulated a lifetime prediction model of nanoscale sintered silver with inputs from accelerated tests and thermomechanical modeling.

In the past, research at the National Renewable Energy Laboratory (NREL) was focused on characterizing the reliability of sintered silver joints synthesized from micron-sized silver particles [1]. Accelerated thermal cycling from -40°C to 150°C was conducted on 50.8-mm x 50.8-mm-footprint test samples, in which Si₃N₄ substrates were bonded to copper baseplates with sintered silver material. The sample synthesis was done at Semikron. A bonding pressure of 30 – 40 MPa was applied that resulted in good quality bonding with minimal voiding. Under thermal cycling, samples survived without failure for 2,300 cycles. A 20% increase in crack area was considered as the failure criterion. More recently, research focus at NREL has shifted to characterizing novel formulations of sintered silver pastes. In collaboration with an industrial partner and Virginia Tech (VT), efforts to evaluate the shear strength and reliability of nano and hybrid sintered silver pastes, in which micron- and nano-sized silver particles are embedded, are ongoing. In this paper, we focus on the mechanical characterization of sintered silver. Sample preparation, synthesis techniques and test procedures are outlined. In the Results section, shear stress values of sintered silver as a function of ambient temperature and applied displacement rates are plotted. The reliability test plan is also described.

SAMPLE DESCRIPTION

1. Sample Geometry

A modified double-lap sample configuration [16, 17], as shown in Fig. 1, was selected to measure the mechanical strength of sintered silver pastes. The sample consists of a 5-mm-thick copper coupon in the middle that is bonded to thinner copper coupons (2-mm-thick) on either end using sintered silver. The simple layout of this sample configuration enables an effective characterization of the joint material without the occurrence of any unintended peel stress at the interfaces. By applying a compressive force on the top of the middle coupon, as shown in Fig. 1, shear forces are developed in the sintered silver joints. The copper coupons were fabricated in the laboratory machine shop with a prescribed surface finish of RMS 16. After fabrication, the coupons were plated with a 4- μ m-thick silver layer. The footprint of the samples was 12.7 mm x 12.7 mm.

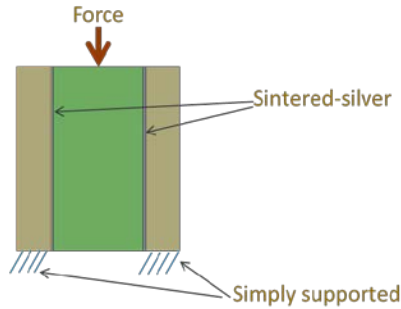


Fig. 1. Double-lap sample configuration for mechanical characterization

2. Sample Synthesis

After plating, the copper coupons were bonded in a double-lap configuration with sintered silver material as described in the previous section. Two types of sintered silver pastes were included in this study. In one set of double-lap samples, the copper coupons were bonded using a sintered silver paste that was purchased from an industrial partner, while the other set of samples was synthesized at VT using a sintered silver paste purchased from NBE Tech.

a. Samples bonded with sintered silver paste purchased from the industry partner

The synthesis of a double-lap sample at NREL using this sintered silver paste was achieved in two stages. First, the paste was applied using a 150- μm -thick stencil printer in a circular pattern with an 8-mm diameter onto a thin copper coupon that was then placed in a slot within a sample holder. To ensure proper alignment within the sample, the thicker middle coupon was carefully dropped on top of the thin coupon. After repeating this procedure for multiple samples, the sample holder was placed inside a solder reflow station. Figure 2 shows the sintering profile that was adopted for this sintered silver paste. Sintering was performed in an inert gas atmosphere, and no pressure was applied on the coupons at any stage of the sintering profile. Once the sintering was completed and a bond formed between the two copper coupons, the entire process was repeated on the other side of the thicker copper coupon to complete the synthesis of one double-lap sample. Figure 3 shows the layout of the different synthesis steps that were followed to make a double-lap sample. After the sintering process, the final bond line thickness was measured to be roughly between 50 μm and 70 μm .

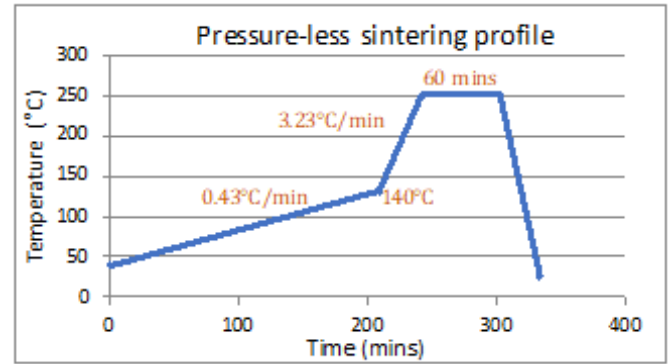


Fig. 2. Sintering profile for sintered silver paste purchased from an industry partner

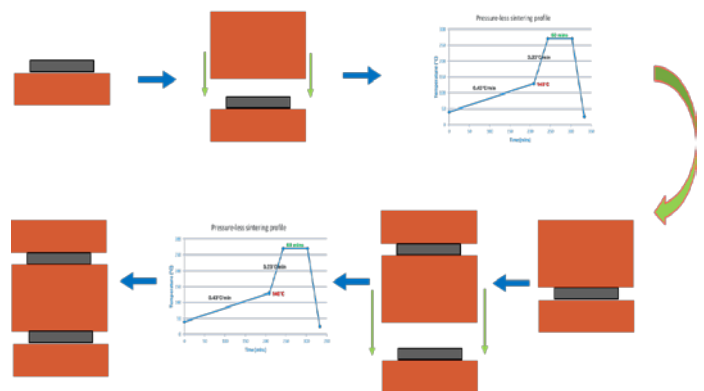


Fig. 3. Synthesis procedure of a double-lap sample

b. Samples synthesized at VT

In addition to using a different sintered silver paste, double-lap samples were synthesized in VT in two different ways – one through a purely pressure-less sintering technique, and the other using a pressure-assisted technique. It is noted here that while this silver paste does not require any sintering pressure as such, the pressure-assisted technique was included in the study to investigate the impact of external bonding pressure on the shear strength of these samples. Samples were made using 3 MPa as well as 10 MPa sintering pressure.

The pressure-less sintering procedure at VT followed a similar pattern as the samples made at NREL. To complete the synthesis of one double-lap sample, each interface was sintered separately, using the profile shown in Fig. 4. A few trials and variations were conducted with the pressure-less as well as the pressure-assisted sintering techniques before finally selecting the sintering profile and the stencil thickness. Unlike the circular pattern at the interface for the samples bonded at NREL, the double-lap samples made at VT employed a square footprint geometry for the material at the interface. The final bond line thickness of the pressure-less and pressure-assisted samples was roughly 80 μm – 100 μm . In this paper, only the

characterization results of samples synthesized using the pressure-less sintering technique are covered.

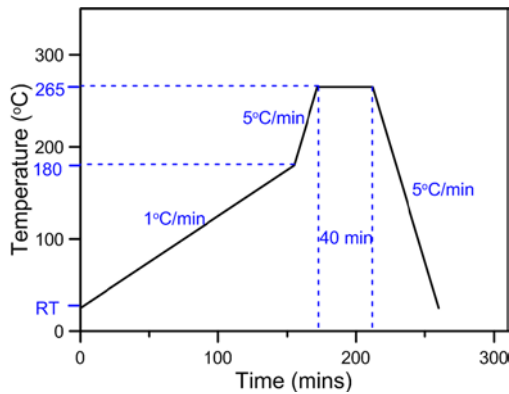


Fig. 4. Sintering profile of samples synthesized at VT

Once the double-lap samples were synthesized, the material bonding quality was assessed using images taken with C-mode scanning acoustic microscopy (C-SAM) at NREL. Figure 5 shows select C-SAM images of double-lap samples made at NREL and VT.

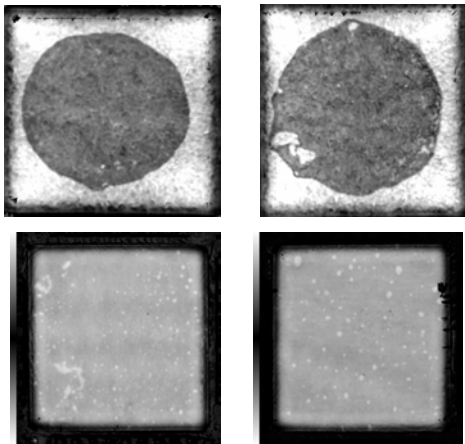


Fig. 5. C-SAM images of double-lap samples synthesized at NREL (top) and VT (bottom)

The actual bonded area of each interface of all the samples were computed using SPIP image analysis software. In general, most of the samples exhibited a decent bond region with a low amount of voiding, however, those samples with high amount of voiding (>30% by area) were omitted from the study.

EXPERIMENTAL SETUP AND TEST PLAN

Shear testing on the double-lap samples was conducted using an Instron 5966 dual column testing system. The double-lap sample configuration and the fixture design allowed operating the Instron system in compression mode to induce shear stresses at the material interfaces. A 10-kN load cell was used to measure loading on the sample, and the resulting displacement at the interfaces was measured using a non-

contact video extensometer. After the fixture was positioned on the base mount, the crosshead beam was slowly jogged downwards until the cylindrical bar connected to the load cell just touched the plunger in the fixture. Once the testing started, loading would be applied to the plunger, which then pushed down the middle coupon, inducing a shear stress at the interface regions. The displacement of the joint material was measured by tracking the relative movement of two white indicator dots in the field of view of the video extensometer. These white dots were marked on the plunger and the sample holder. The Instron system also consisted of a thermal oven that allowed testing to be conducted at different ambient temperatures. The temperature range of the oven was from -100°C to 300°C. A picture of the Instron test system with the thermal oven is shown in Fig. 6.

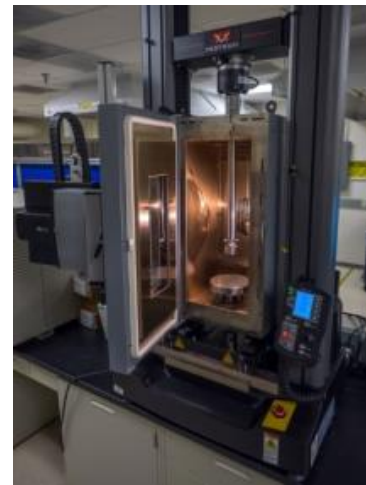


Fig. 6. Instron 5966 dual column test system

In this study, the double-lap samples were characterized at three different displacement rates: 10^{-2} mm/s, 10^{-4} mm/s, and 10^{-5} mm/s, and at three different ambient temperatures: -40°C, 30°C, and 200°C. The intent behind choosing these rates was to simulate quasi-static loading conditions at the joint interfaces, thereby qualifying the results obtained from these tests to be applicable in scenarios such as thermal cycling. In a study on developing a constitutive model for SAC solders [18], the authors used a closed-loop mechanism that monitored and controlled the displacement rates at the solder joint interfaces of double-lap samples to compensate for the compliance in the load train and to accommodate the rate-dependent behavior of solder joints. However, in this study, the testing rates were controlled at the Instron crosshead and it was assumed that the actual effective displacement rates at the sample interfaces were the same. For each instance of a displacement rate and temperature, a total of four samples were tested and the average shear stress values are reported in this paper.

RESULTS AND DISCUSSION

The direct output of shear testing on a double-lap sample using an Instron test equipment is the load-displacement curve, shown in Fig. 7. The two peaks in the figure denote the failure points of the two interfaces in the sample, and only the results obtained up to the first failure point are considered for further analysis. In the case of a few samples, the load-displacement graph exhibited only a single peak, which could lead to the misconception that only one interface failed. However, both interfaces were observed to shear off for these samples during the test. To observe the failure mechanism in the sintered silver material, a test run was conducted on a sample synthesized at NREL (with sintered silver paste purchased from the industrial partner). Before testing, the sample was cross-sectioned, and the interface region was closely captured using a digital microscope. The resulting image obtained is shown in Fig. 8. Clearly, a cohesive fracture mechanism within the sintered silver layer can be observed in this image.

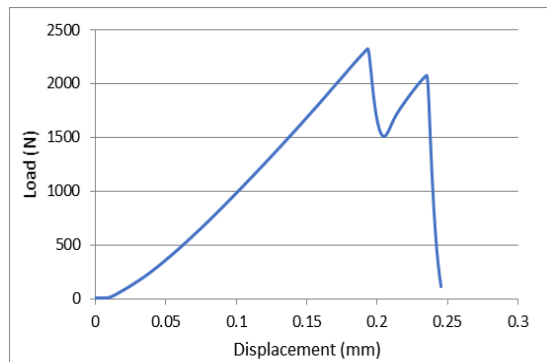


Fig. 7. Load-displacement graph

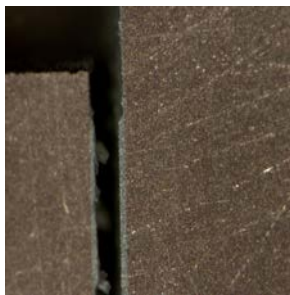


Fig. 8. Cohesive fracture observed in the sintered silver layer of a double-lap samples under shear testing

For a given sample, the load information obtained from the tests were converted to stress results using Eq. (1).

$$\sigma = \frac{F}{A} \quad (1)$$

where,

F is the load

A is the total area of both sample interfaces measured from C-SAM images using SPIP

1. Pressure-less samples (NREL)

As described above, the double-lap samples synthesized at NREL were bonded using a sintered silver paste purchased from an industrial partner. These samples were synthesized using the profile as shown in Fig. 2, and the C-SAM images of these samples showed very minimal voiding at the interface regions. The average values of the peak shear stress of these samples are plotted in Fig. 9. The error bars represent the standard deviation of the shear stress results. At each displacement rate, there is more than a 50% drop in the shear stress value as ambient temperature is increased from room temperature (RT) to 200°C. Also, at a given temperature, a decrease in the applied displacement rate leads to a 40% – 50% drop in the shear stress of the sintered silver joint. The wide variation in the individual results averaged to obtain the plotted values, particularly at RT, could be likely due to differences in the bond shape between the samples. Although the paste was printed in a circular shape, it spread out and, in a few instances, did not conform to a circular shape.

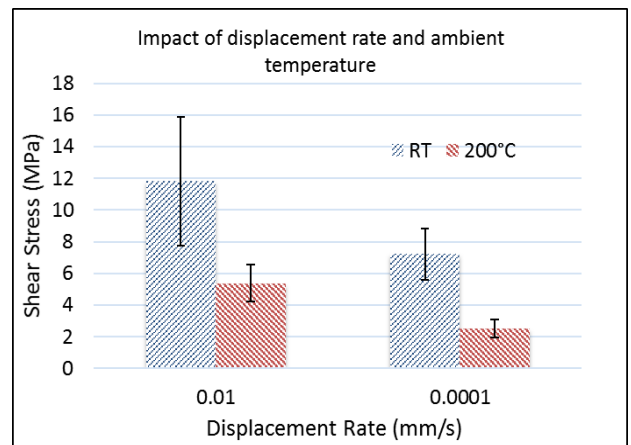


Fig. 9. Shear stress values of samples synthesized at NREL

In addition to the mechanical characterization on samples sintered at 250°C, shear testing was conducted on a few samples synthesized with a sintering temperature of 270°C. A comparison of shear stress results between samples sintered at 250°C and 270°C is given in Fig. 10. Although a significant increase in shear stress values cannot be observed, these results indicate that on an average, a higher sintering temperature led to a slightly increased inter-particle bonding force within the sintered silver paste.

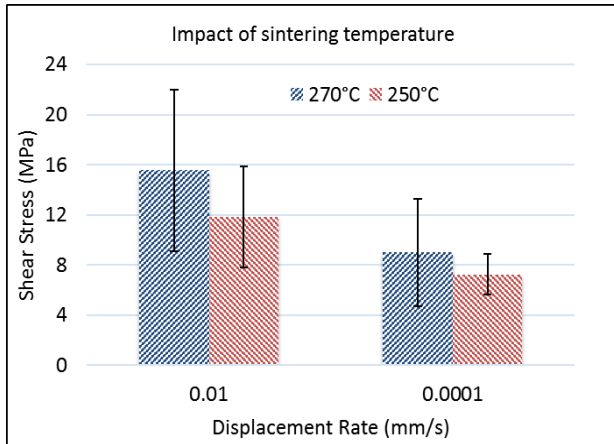


Fig. 10. Comparison of samples sintered at 250°C and 270°C

2. Pressure-less samples (VT)

Similar to the samples synthesized at NREL, mechanical characterization was conducted on double-lap samples fabricated at VT using the sintered silver paste from NBE Tech. For a given displacement rate and temperature, multiple samples were characterized, and the shear stress results were computed from the resulting load-displacement graphs. Figure 11 shows a plot of the impact of displacement rate and ambient temperature on the shear stress values of these samples. As seen in the figure, there does not exist much difference in the shear stress values between the samples tested at -40°C and RT. However, a considerable drop occurs when the ambient temperature is raised to 200°C, a trend that was observed in the samples synthesized at NREL. The fall in shear stress values with increasing temperature could be attributed to creep deformation becoming predominant at higher temperatures, which diminishes the material resistance to failure. Also, the applied displacement rate did not have a significant impact on the shear stress values at -40°C and RT. Only when the ambient temperature was increased to 200°C did the silver paste exhibit a strong rate dependence.

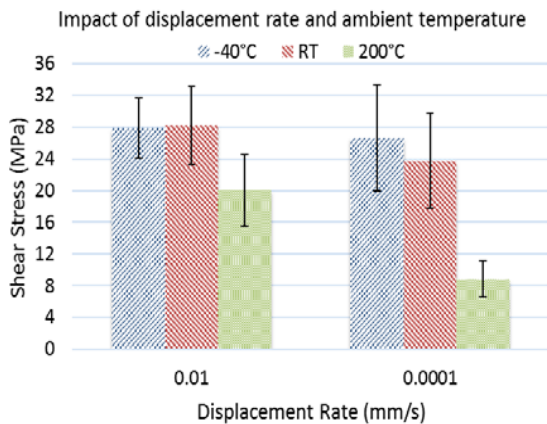


Fig. 11. Mechanical characterization results of samples synthesized at VT

While the decrease in shear stress of a sintered silver bond with rising temperature and decreasing displacement rate, as observed in this study, conforms to the trends that exist in the open literature [5, 19], more work is required to ascertain the exact behavior of the silver paste at the microstructural level under these conditions.

FUTURE WORK

Research study in characterizing the silver pastes under the displacement rate of 10^{-5} mm/s is currently ongoing. Conducting shear tests at extremely slow rates and at elevated temperatures is a challenging task and a cautious approach in setting up the test equipment needs to be adopted. Shear stress versus shear strain graphs will be created from the existing set of data and the failure behavior of the sintered silver pastes in these tests, whether it is brittle or ductile, will be investigated. Preliminary characterization tests of double-lap samples synthesized using pressure-assisted sintering process produced promising results. A rigorous study of the shear behavior of these samples at multiple strain rates and temperatures will be conducted.

In addition to mechanical characterization to determine the shear properties of sintered silver, a reliability evaluation study through accelerated thermal cycling will be initiated. Round samples of 25.4-mm-diameter with copper and Invar coupons bonded using sintered silver pastes were fabricated. Copper and Invar coupons were selected for this study to create a large coefficient of thermal expansion mismatch across the sintered silver joint. C-SAM images of these samples show negligible amounts of voiding in the joint region. These round samples will be subjected to a thermal cycle going from -40°C to 200°C and will be imaged using C-SAM periodically to monitor the occurrence of any failure mechanisms such as crack initiation and propagation. Also, lifetime prediction models will be developed by correlating the experimental results obtained from thermal cycling with strain energy density/J-integral results computed through finite element modeling analysis.

CONCLUSIONS

This paper focused on characterizing the shear behavior of two different sintered silver pastes bonded in a double-lap sample configuration. Samples were synthesized at NREL and VT using pressure-less sintering techniques and shear testing was conducted on these samples in an Instron testing system at NREL. Mechanical characterization was done at multiple temperatures and applied displacement rates, and the maximum values of shear stress obtained in each case are reported. In general, shear stress of the silver pastes in this study dropped with increasing temperature and decreasing displacement rates. Additional experiments will be conducted to infer the behavior of these pastes at the microstructural scale under these conditions. Future work in this project includes conducting thermal cycling experiments to evaluate reliability and developing thermomechanical models. Cycles-to-failure results

obtained from accelerated tests will be correlated with strain energy density/J-integral values computed through modeling to formulate a lifetime prediction model for sintered silver.

ACKNOWLEDGEMENTS

This work was authored by Alliance for Sustainable Energy, LLC, the manager and operator of the National Renewable Energy Laboratory for the U.S. Department of Energy (DOE) under Contract No. DE-AC36-08GO28308. Funding provided by Susan Rogers, Technology Manager for the Electric Drive Technologies Program, Vehicle Technologies Office, U.S. Department of Energy Office of Energy Efficiency and Renewable Energy (EERE). The views expressed in the article do not necessarily represent the views of the DOE or the U.S. Government. The U.S. Government retains and the publisher, by accepting the article for publication, acknowledges that the U.S. Government retains a nonexclusive, paid-up, irrevocable, worldwide license to publish or reproduce the published form of this work, or allow others to do so, for U.S. Government purposes. We would also like to thank Andrew Wereszczak (Oak Ridge National Laboratory) for his guidance and insightful comments on sample preparation and design for reliability evaluation study.

REFERENCES

1. P. Paret, D. DeVoto, and S. Narumanchi, "Reliability of Emerging Bonded Interface Materials for Large-Area Attachments," *IEEE Trans. Compon. Packag. Manufac. Technol.*, vol. 6, no. 1, pp. 40–49, Jan. 2016.
2. J. Bai, Z. Zhang, J. Calata, and G.-Q. Lu, "Low-Temperature Sintered Nanoscale Silver as a Novel Semiconductor Device-Metallized Substrate Interconnect Material," *IEEE Trans. Comp. Packag. Technol.*, vol. 29, no. 3, pp. 589-593, 2006.
3. C. Gobl, "Low Temperature Sinter Technology Die Attachment for Power Electronic Applications," *Proc. CIPS*, p. 327, Nuremberg, 2010.
4. K. Siow, "Are Sintered Silver Joints Ready for Use as Interconnect Material in Microelectronic Packaging?" *J. of Electron. Mater.*, vol. 43, No. 4, pp. 947–961, Jan. 2014.
5. R. Khazaka, L. Mendizabal, and D. Henry, "Review on Joint Shear Strength of Nano-Silver Paste and its Long-Term High Temperature Reliability," *J. of Electron. Mater.*, vol. 43, No. 7, pp. 2459–2466, Jul. 2014.
6. J. Li, C. Johnson, C. Buttay, W. Sabbah, and S. Azzopardi, "Bonding Strength of Multiple SiC Die Attachment prepared by Sintering of Ag Nanoparticles," *J. of Mater. Proc. Tech.*, vol. 215, pp. 299-308, Jan. 2015.
7. V. Caccuri, X. Milhet, P. Gadaud, D. Bertheau, and M. Gerland, "Mechanical Properties of Sintered Ag as a New Material for Die Bonding: Influence of the Density," *J. of Electron. Mater.*, vol. 43, No. 12, pp. 4510–4514, Dec. 2014.
8. J. Kähler, N. Heuck, G. Palm, A. Stranz, A. Waag, and E. Peiner, "Die-Attach for High-Temperature Applications Using Fineplacer-Pressure-Sintering (FPS)," *3rd Electronics System Integration Technology Conference ESTC*, pp. 1-5, Berlin, 2010.
9. S. Chua, K. Siow and A. Jalar, "Effect of Sintering Atmosphere on the Shear Properties of Pressureless Sintered Silver Joint," *36th International Electronics Manufacturing Technology Conference*, pp. 1-6, Johor Bahru, 2014.
10. S. Egelkraut, L. Frey, M. Knoerr, and A. Schletz, "Evolution of Shear Strength and Microstructure of Die Bonding Technologies for High Temperature Applications during Thermal Aging," *2010 12th Electronics Packaging Technology Conference*, pp. 660-667, Singapore, 2010.
11. J. Bai and G-Q Lu, "Thermomechanical Reliability of Low-Temperature Sintered Silver Die Attached SiC Power Device Assembly," *IEEE Trans. Dev. Mat. Reliab.*, vol. 6, no. 3, pp. 436–441, Sep. 2006.
12. S. Zhao, X. Li, Y-H. Mei, and G-Q. Lu, "Study on High Temperature Bonding Reliability of Sintered Nano-Silver Joint on Bare Copper Plate," *Microelectron. Reliab.*, vol. 55, iss. 12, part A, pp. 2524-2531, Dec. 2015.
13. M. Knoerr, S. Kraft and A. Schletz, "Reliability Assessment of Sintered Nano-Silver Die Attachment for Power Semiconductors," *2010 12th Electronics Packaging Technology Conference*, pp. 56-61, Singapore, 2010.
14. P. Rajaguru, H. Lu, and C. Bailey, "Sintered Silver Finite Element Modelling and Reliability Based Design Optimization in Power Electronic Module," *Microelectron. Reliab.*, vol. 55, iss. 6, pp. 919-930, May 2015.
15. F. Henaff, S. Azzopardi, E. Woigard, T. Youssef, S. Bontemps, and J. Joguet, "Lifetime Evaluation of Nanoscale Silver Sintered Power Modules for Automotive Application based on Experiments and Finite-Element Modeling," *IEEE Trans. Dev. Mater. Reliab.*, vol. 15, no. 3, pp. 326-334, Sep. 2015.
16. D. Mendels, S. Page, Y. Leterrier, J. Manson, and J. Nairn, "A Modified Double Lap-Shear Test as a Mean to Measure Intrinsic Properties of Adhesive Joints," *9th European Conference on Composite Materials*, United Kingdom, 2000.
17. G. Challita, R. Othman, P. Casari, and K. Khalil, "Experimental Investigation of the Shear Dynamic Behavior of Double-Lap Adhesively Bonded Joints on a Wide Range of Strain Rates," *Int. Jour. Adhesion and Adhesives*, vol. 31, iss. 3, pp. 146-153, Apr. 2011.
18. D. Bhate, D. Chan, G. Subbarayan, T. Chiu, V. Gupta, and D. Edwards, "Constitutive Behavior of Sn3.8Ag0.7Cu and Sn1.0Ag0.5Cu Alloys at Creep and Low Strain Rate Regimes," *IEEE Trans. Comp. Packag. Tech.*, vol. 31, no. 3, pp. 622-633, Sep. 2008.
19. X. Li, G. Chen, X. Chen, G-Q. Lu, L. Wang, and Y-H. Mei, "Mechanical Property Evaluation of Nano-Silver Paste Sintered Joint using Lap-Shear Test," *Solder. Surf. Mount Tech.*, vol. 24, iss. 2, pp. 120-126, 2012.